Performance comparison of Nuclear Magnetic Resonance and FerriMagnetic Resonance field markers for the control of low-energy Synchrotrons

IOP Conf. Series: Journal of Physics: Conf. Series **1065** (2018) 052022 doi:10.1088/1742-6596/1065/5/052022

Performance comparison of Nuclear Magnetic Resonance and FerriMagnetic Resonance field markers for the control of low-energy Synchrotrons

Christian Grech[1,2], Anthony Beaumont[2,3], Marco Buzio[2], and Nicholas Sammut[1]

[1] University of Malta, MSD 2080, Malta
[2] CERN, European Organization for Nuclear Research, Geneva, Switzerland
[3] EPFL, École polytechnique fédérale de Lausanne, Lausanne, Switzerland

E-mail: christian.grech.12@um.edu.mt

Abstract. A field marker is a magnetic field sensor used in synchrotrons, which provides a digital trigger when the magnetic field reaches a pre-set threshold. This paper describes the results of an in-situ measurement performed on the Extra Low ENergy Antiproton (ELENA) decelerator's main bending dipoles at the European Organization for Nuclear Research (CERN). It compares the dynamic behavior of Nuclear Magnetic Resonance (NMR) markers and FerriMagnetic Resonance (FMR) markers in different magnetic fields for the operation of these sensors in low-energy synchrotrons.

1. Introduction

In synchrotrons, the knowledge of the magnetic field value of the bending dipoles is essential for beam control. A real-time magnetic measurement system called the B-train is used to transmit the magnetic field $B(t)$ to users, including mainly the Low-Level Radio Frequency (RF) cavity system. At CERN, $B(t)$ is distributed using the B-train system in the Low Energy Ion Ring (LEIR), the Proton Synchrotron Booster (PSB), the Proton Synchrotron (PS), the Super Proton Synchrotron (SPS), the Antiproton Decelerator (AD) and the Extra Low ENergy Antiproton (ELENA) ring.

A combination of induction coils and field markers is used to measure the magnetic field. A static induction coil, shaped to follow the nominal beam orbit, generates a voltage $V_c(t)$, proportional to the field time variation, which is acquired using an analog-to-digital converter. This voltage is integrated in order to calculate the magnetic field $B(t)$. A field marker that triggers a digital signal at $t = t_0$ when $B = B_0$ is then used as an integration constant. Magnetic markers are used to improve the B-train's accuracy and reproducibility, as they consider the remanent field and correct the gain when using two markers [2]. The calculation for the average $B(t)$ is noted in Equation 1, where A is the effective surface area of the coil:

$$B(t) = \frac{1}{A}\int_{t_0}^{t} V_c\, dt + B_0 \tag{1}$$

2. Magnetic Resonance-based field markers

Any sensor capable of measuring absolute field values could be considered, in principle, to take the role of a marker. The main requirement for stable beam operation is a long-term reproducibility of the order of 20 μT or better, under a wide range of field and field ramp rate levels, which is difficult to achieve with commonly used sensors such as Hall probes [1]. In the case of the ELENA B-train system, the choice was narrowed down to Nuclear Magnetic Resonance (NMR) and FerriMagnetic Resonance (FMR) sensors, due to their proven performance and practicality in application.

Magnetic resonance is based on the spin state change of the nuclei (for NMR) or electrons (for FMR) in the presence of an external field B_0. The resonance (jump between the two spin states) occurs when an excitation RF wave with frequency f_0 having a magnetic component perpendicular to B_0 corresponding to the difference between the energy of the two states is supplied to the sample:

$$f_0 = \frac{\gamma}{2\pi} B_0 \tag{2}$$

where γ is the gyromagnetic ratio. NMR is a primary metrological reference, providing the best accuracy for a wide magnetic field range [3], with a gyromagnetic ratio $\gamma_{NMR}/2\pi = 42.57608$ MHz/T for ^1H. The main limitations of NMR, i.e. a homogeneous field and low ramp rate, can be partially overcome by FMR markers. In the case of the ELENA machine, the FMR sensor used is a band-pass Yttrium Iron Garnet (YIG) filter, where the resonating sample is a Gallium-doped YIG sphere of 0.36 mm diameter, with a gyromagnetic ratio $\gamma_{FMR}/2\pi = 28.02495$ GHz/T (for an isolated electron). Due to the small sample sizes, comparatively higher spin density and shorter relaxation time, considerable field gradients and field ramp rates can be tolerated [4]. On the other hand, this FMR sensor is optimized for a field of 60 mT. Figure 1 shows the NMR and FMR signals generated when the field level corresponding to the resonant frequency is reached. In the B-train system, a peak detector subsequently detects the minimum peak of the signal and generates a trigger signal.

A previous study [5] has already confirmed that the NMR field marker is a viable option for low-fields at the ELENA ring. Another study [6] investigates the static and the dynamic behavior of the FMR sensor at one field level, 95 mT, where the repeatability is found to be better than 20 μT. Beaumont [7] investigates the performance of NMR and FMR field markers for the PS ring and reports a reproducibility of 5 μT and 6 μT respectively using a combined-function

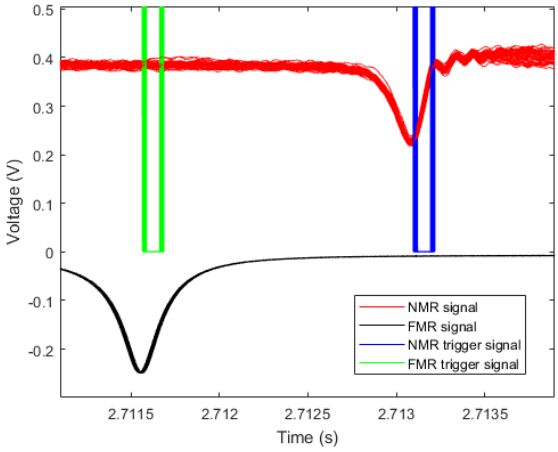

Figure 1. FMR and NMR signals with the corresponding generated trigger signals at 200 mT with a ramp rate of 368 mT/s

magnet at different field levels and unspecified ramp rates. This study focuses on the relative dynamic performances of the two sensors when operating at five different field levels, whilst investigating the performance of the FMR sensor when operated outside its optimal conditions.

3. Experimental Setup

The ELENA reference dipole, connected in series with the ring dipole magnets, is used for the test, with the magnetic field measurements carried out using the PT2025 teslameter by Metrolab Instruments [8] and National Instruments USB card (USB-6366) with an acquisition rate of 1 MHz. The probes are installed in the centre of the magnet, and measurements are taken from both probes simultaneously. An independent peak detection card is used for each magnetic resonance signal in order to generate a trigger signal at the minimum peak. The complete setup in the magnet is illustrated in Figure 2.

This study investigates the performance of these two sensors at the field range of 43 mT to 200 mT, where the lower limit is the NMR's specified lowest range. The ramp rates vary from 53 mT/s to 750 mT/s. Following the analysis of 100 signals for the 14 different field (B) and field ramp rate ($\dot{B}$) parameters, the repeatability of one sigma (σ) of the trigger signal generation $\sigma_{t_{NMR}}$, is found using the standard deviation of the trigger time. Comparison of subsequent cycles requires the assumption that the magnetic history is repeatable as a function of time, as it was verified independently. Furthermore, the equivalent value in tesla $\sigma_{B(t_{NMR})}$ is calculated by multiplying $\sigma_{t_{NMR}}$ with the ramp rate. The reproducibility ($\bar{\sigma}_{B(t_{NMR})}$) is calculated by finding the mean of the standard deviation in the trigger time generation, in order to compare the performance of the FMR and NMR sensors at three different $(B, \dot{B})$ sections. Finally, the delay between the FMR and NMR trigger signal ($\Delta t_{NMR-FMR}$) is measured to characterize the effect of the NMR probe's inbuilt filter at different field levels and ramp rates.

4. Results

Table 1 shows the results obtained at three field levels. In general, reproducibility improves at high field levels and low ramp rates. The biggest difference in the reproducibility of the two sensors is noticed at the lowest field values. This can be attributed to the FMR sensor's saturation magnetization and the fact that at lower fields, the FMR signal becomes wider, and hence leads to imprecise peak detection. An independent t-test finds no statistical significant difference between the performance of the FMR and NMR sensors for $B \leq 45$ mT at a level of marginal significance $p < 0.05$. At the two other field/ramp rate levels, the difference in performance of the two sensors is also found to be statistically insignificant at $p < 0.05$.

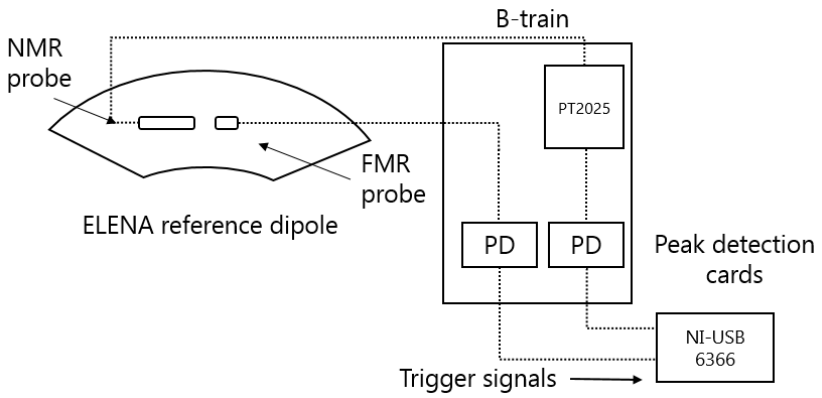

Figure 2. Experimental setup

Table 1. Trigger signal repeatability for FMR and NMR sensors

B (mT)	$\dot{B}$ (mT/s)	$\sigma_{t_{NMR}}$ [μs]		$\sigma_{B(t_{NMR})}$ [μT]		$\bar{\sigma}_{B(t_{NMR})}$ [μT]		$\Delta t_{NMR-FMR}$ (ms)
		NMR	FMR	NMR	FMR	NMR	FMR	
43.0	53.3	42.0	63.3	2.2	3.4			0.62
	93.5	37.4	54.1	3.5	5.1			0.72
45.0	53.3	57.8	205	3.1	10.9	4.7 ± 2.6	11.3 ± 8.5	1.00
	93.5	65.9	129	6.2	12.1			0.30
	102	83.0	246	8.4	25.0			1.09
70.0	368	8.3	6.3	3.1	2.3			0.05
	498	6.8	4.7	3.4	2.3			0.01
	748	7.5	3.7	5.6	2.8			0.10
100	368	8.0	7.8	3.0	2.9	3.7 ± 1.0	2.8 ± 0.4	0.24
	498	6.3	6.2	3.1	3.1			0.28
	748	5.5	4.2	4.1	3.2			0.23
200	368	6.8	8.7	2.5	3.2			1.52
	498	6.1	5.2	3.0	2.6	3.3 ± 0.9	2.8 ± 0.3	2.03
	748	5.6	3.6	4.2	2.7			1.05

5. Conclusion

Under the present test conditions, no sensor is clearly found to outperform the other on a statistical basis; the choice should therefore be informed by considerations of cost and practicality. The commercial NMR system used is relatively expensive, although, if required it can also provide high-quality DC measurements. Moreover, the probe could be adapted to work in stand-alone mode without the teslameter unit, reducing considerably the cost. On the other hand, FMR sensors are made at CERN and are still undergoing considerable R&D; they have the advantage of working in the multi-GHz frequency range, leading to considerable noise immunity and clean signals, as seen in Figure 1. In the end, since the NMR sensor results to be slightly more repeatable across all target field levels and ramp rates, it is chosen as the best candidate for the operation of the ELENA ring.

Acknowledgments

The authors would like to thank Martino Colciago, Lucio Fiscarelli, David Giloteaux, Marco Roda and Joseph Vella Wallbank for their contribution to the B-train system.

References

[1] M. Pezzetta, G. Bazzano, E. Bressi, L. Falbo, M. Pullia, C. Priano *et al.*, B-Train Performances at CNAO *Proceedings of IPAC 2011, San Sebastian, Spain.*
[2] Caspers F and Cornuet D 1999 NMR Probe as a Field Marker in a Quadrupole *Eleventh International Magnet Measurement Workshop (IMMW).*
[3] Reymond C 1998 Magnetic Resonance Techniques *CERN Accelerator School: Measurement and Alignment of Accelerator and Detector magnets.*
[4] Caspers F 1994 *FerriMagnetic Resonance: A method to measure magnetic fields in accelerator environment* (Geneva: CERN).
[5] Grech C et al. 2018 Metrological Characterization of Nuclear Magnetic Resonance Markers for Real-time Field Control of the CERN ELENA Ring Dipoles, *IEEE Sensors Journal* **18** 10.1109/JSEN.2018.2842710.
[6] Arpaia P et al. 2012 Metrological Performance of a Ferrimagnetic Resonance Marker for the Field Control of the CERN Proton Synchrotron, *IEEE Trans. on Applied Superconductivity* **22** 9001904
[7] Beaumont A 2008 *Magnetic field markers of the B-Train for the Proton Synchrotron accelerator* (Geneva: CERN)
[8] PT2025 NMR Teslameter User Manual 2003 METROLAB Instruments SA.